Stationary and transient processes in the region of overlap of nuclear and electron magnetic resonance

V. A. Ignatchenko, V. K. Mal'tsev, and V. I. Tsifrinovich

L. V. Kirenskiĭ Institute of Physics, Siberian Branch of the Academy of Sciences of the USSR, Krasnoyarsk
(Submitted 13 January 1978)
Zh. Eksp. Teor. Fiz. **75**, 217–227 (July 1978)

A theoretical study is reported of the effect of inhomogeneities on the shape of the absorption line and the properties of FMR and AFMR when the frequencies of nuclear and electron magnetic resonance are equal. It is shown that the shift of the FMR and AFMR resonance fields is proportional to the real part of nuclear susceptibility. Thin ferromagnetic films have been used to investigate experimentally the stationary and some of the transient phenomena in the region of overlap of NMR and FMR. It was shown that the experiments on stationary phenomena could be used to obtain separately the real and imaginary parts of the nuclear susceptibility.

PACS numbers: 76.50.+g

1. INTRODUCTION

The region in which the frequencies of nuclear magnetic resonance and of ferro- and antiferromagnetic resonance are equal corresponds, in one sense, to an extremal state of the electron-nuclear (EN) magnetic system and has attracted the attention of both theoreticians and experimenters for a considerable length of time.[1] Thus, studies have been carried out of the EN eigenfrequencies, without taking relaxation into account, in both ferromagnetic[2,3] and antiferromagnetic[4] materials. It was found experimentally[5] that there was a shift of the FMR resonance field in the NMR and FMR overlap region. It was also shown[6] that, when the electron relaxation parameter was large, the EN eigenfrequencies tended to cross rather than move apart. Various stationary and transient phenomena have been examined[7-10] under conditions of overlap of NMR and FMR, and the phenomenon of electron nuclear magnetic resonance (ENMR), which was predicted theoretically by Ignatchenko and Tsifrinovich,[8] has been confirmed experimentally.[11,12]

The theoretical studies performed so far have shown that, in some ferromagnetic and antiferromagnetic materials of the "easy plane" type, the FMR (AFMR) frequency $\omega_e(H)$ can be reduced down to the NMR frequency ω_n (so far, this situation has been achieved experimentally only in thin ferromagnetic films). The nature of the phenomena that arise in the region of overlap of the nuclear and electron magnetic resonances is wholly determined by the relation between three parameters, namely, the dynamic EN interaction parameter ω_q and the electron and nuclear relaxation parameters Γ_e and Γ_n. The parameter ω_q represents the "repulsion" between the eigenfrequencies of EN oscillations in the absence of relaxation, and Γ_n and Γ_e are the half-widths of the noninteracting NMR and FMR (AFMR) lines. For antiferromagnetic materials of the "easy plane" type, $\omega_q \approx \gamma_e(A\mu H_E)^{1/2}$, where H_E is the exchange field,[1] and the other symbols have their usual meanings.[8] In the case of ferromagnetic materials, ω_q depends on the shape of the specimen[2] and reaches its maximum value in the limit of maximum asymmetry in the plane of precession: $\chi^0_{ey} \ll \chi^0_{ex}$, where χ^0_{ex} and χ^0_{ey} are the static electronic susceptibilities along the x and y axes, respectively. To be specific, we shall confine our attention to this particular situation, in which case $\omega_q = \gamma_e(A\mu M/\chi^0_{ey})^{1/2}$.

When $\omega_q > |\Gamma_e - \Gamma_n|$, the eigenfrequencies of the EN oscillations are pushed apart, whereas the opposite inequality ensures that they cross.[8] In magnetic materials, it is usually found that $\Gamma_e \gg \Gamma_n$ and, therefore, the criterion for the crossing of eigenfrequencies depends on the relation between Γ_e and ω_q. When $\omega_q \gg \Gamma_e$, there are two coupled EN modes at the point $\omega_e(H) = \omega_n$, with complex frequencies

$$\tilde{\omega}_\pm \approx \omega_n \pm \frac{1}{2}(\omega_q^2 - \Gamma_e^2)^{1/2} + i\Gamma_e/2. \tag{1}$$

The leading features of both stationary and transient pehnomena are then determined by the dynamic shift of frequencies $\omega'_\pm$, which is a maximum at the point of crossing.

When $\omega_q \ll |\Gamma_e|$, the EN vibrations can definitely be separated into electron-like and nuclear-like. The complex frequencies of these oscillations, $\tilde{\omega}_e$ and $\tilde{\omega}_n$, are related by the expression $|\tilde{\omega}_e\tilde{\omega}_n|^2 = (\omega_e^2 - \omega_q^2)\omega_n^2$. The dynamic shift of the frequency of the nuclear-like vibrations is given by $D = \frac{1}{2}\gamma_n A^2\chi'_{ex}\mu$, and is zero at the point of intersection, whereas the attenuation Γ_n is augmented by $\Gamma_\varkappa = \frac{1}{2}\gamma_n A^2\chi''_{ex}\mu$,[9] where χ'_{ex} and χ''_{ex} are the real and imaginary parts of electronic susceptibility χ_{ex}. The quantity $\Gamma_\varkappa$ is a measure of the reciprocal of the electron-nuclear relaxation time i.e., the relaxation of the nuclear system due to the decay of electronic magnetization. The maximum values of $\Gamma_\varkappa$ and D are determined to within the factor of $\frac{1}{2}$ by the renormalized dynamic *EN* interaction parameter $\omega_q^2/4\Gamma_e$.

The absorption of energy in the *EN* magnetic system was investigated by Gossard *et al.*[13] in the case of well separated NMR and FMR frequencies. The effect of strong inhomogeneous NMR broadening (exceeding the FMR linewidth) on the absorption of energy in the region of overlap between NMR and FMR was analyzed by Botvinko and Ivanov.[7] Ignatchenko and Tsifrinovich[8] have examined the case where $\Gamma_e \gg \Gamma_n$, which is characteristic for magnetic materials. When $\Gamma_e \ll \omega_q$, the absorption line plotted on a frequency scale takes the form of two resolved peaks corresponding to the two modes of coupled EN vibrations. When $\Gamma_e \gg \omega_q$, the situation is essentially modified. Here, scanning along the frequency scale should reveal the presence of an inverted and amplified NMR signal against the background of the broad FMR line. This phenomenon has been predicted theoretically[8] and is called the electron-nuclear magnetic resonance (ENMR). It is a general effect in the case of interacting resonances and can be used to amplify a weak and narrow resonance when it overlaps a strong and broad resonance.

By weak resonance, we understand resonance which does not directly intereact (or interacts weakly) with the high-frequency field. The inversion of the NMR signal is connected with the fact that the electron signal induced by the nuclear system is in antiphase with the electron signal induced by the high-frequency field. The additional amplification of the EMR line is connected with the increase in the electronic susceptibility during EMR. The relative size of the inverted nuclear signal is governed by the parameter

$$(P_{max}-P_{min})/P_{min}=\omega_q^2/4\Gamma_e\Gamma_n. \quad (2)$$

In the case of a strong nuclear signal ($\omega_q^2/4\Gamma_e\Gamma_n>1$), the half-width of the inverted nuclear signal in ENMR is determined by the electron-nuclear relaxation parameter $\Gamma_\varkappa$ (at the crossing point, $\Gamma_\varkappa=\omega_q^2/4\Gamma_e$). For a weak nuclear signal ($\omega_q^2/4\Gamma_e\Gamma_n<1$), the ENMR phenomenon is most clearly defined because the shape of the inverted nuclear line is then practically the same as the shape of the undisturbed NMR line.

It is clear from this brief review that most of the phenomena that occur in the region of overlap between NMR and FMR have already been tackled theoretically and the first steps have been taken toward its experimental study. There are, however, several unresolved questions, some of which will be examined in the present paper.

The most immediate problem is to generalize the ENMR theory developed earlier for ferromagnetic materials[8] to the case of antiferromagnetic materials. In Sec. 2, we give general expressions for the complex susceptibility of the system, which describe ENMR in both ferromagnetic and antiferromagnetic materials with an easy plane. Macroscopic and microscopic inhomogeneities are then taken into account, and an analysis is given of their effect on the ENMR line shape. Particular attention is devoted to the so-called weak nuclear signal produced in our experiments. We then investigate theoretically the scanning of EMR overlapping NMR by varying the magnetic field rather than the frequency. This question has been subject to some misunderstanding in the literature, and this must be resolved. It will be shown below that field scanning can be used to develop a new method for investigating NMR.

Finally, we shall briefly examine the influence of inhomogeneities in magnetic anisotropy on ENMR signal parameters.

Section 3 reports experimental results obtained for thin ferromagnetic films at liquid nitrogen and room temperatures.

2. THEORY

For both ferromagnetic and antiferromagnetic materials, the susceptibility of the EN magnetic system in the direction of polarization of the high-frequency field is given by

$$\chi=\frac{\chi_e-2qA\chi_e\chi_n+\chi_n}{1-(qA)^2\chi_e\chi_n}\approx\frac{\chi_e}{1-(qA)^2\chi_e\chi_n}, \quad (3)$$

where χ_e and χ_n are the undisturbed electronic and nuclear susceptibilities, given by

$$\chi_e=\chi_e^0\frac{\omega_e^2}{2\Gamma_e\omega}\frac{t-i}{t^2+1},\quad t=\frac{\omega_e^2-\omega^2}{2\Gamma_e\omega},$$
$$\chi_n=\chi_n^0\frac{\omega_n^2}{2\Gamma_n\omega}\frac{\delta-i}{\delta^2+1},\quad \delta=\frac{\omega_n^2-\omega^2}{2\Gamma_n\omega}; \quad (4)$$

$q=1$ for ferromagnetic materials and $q=(2\alpha_e\alpha_n)^{-1}$ for antiferromagnetic materials; α_e and α_n are the angles at which the electronic and nuclear sublattices are inclined, and χ_e^0 and χ_n^0 are the static susceptibilities of the electronic and nuclear systems in the direction of polarization of the high-frequency field. (We assume that the high-frequency field **h** is polarized at right angles to the constant field H; in particular, it lies along the x axis for the ferromagnetic material and in the easy plane in the antiferromagnetic material.)

The approximation used in (3) corresponds to the neglect of direct interaction between the nuclear system and the high-frequency field (in comparision with the stronger interaction through the electron magnetic system). This approximation has, in fact, been used in the literature[8-12] to investigate all the effects in ferromagnetic materials. The approximation remains valid for antiferromagnetic media. For a given value of ω_e (H), the absorption line $P(\omega)=\omega\chi''h^2/2$, plotted as a function of frequency, is described by the same expression for both ferromagnetic and antiferromagnetic materials. All the results obtained previously for ferromagnetic media are, therefore, equally valid for antiferromagnetic materials.

We shall now consider the effect of nonuniformity of the field H_n at the nuclei on the ENMR line shape. In general, this problem must be solved by the method of random functions, and the result[14] turns out to depend on the ratio of the inhomogeneity correlation range r_0 and the effective range r_α of the exchange interaction. However, we shall confine our attention to the two limiting situations involving "macroscopic" and "microscopic" inhomogeneities, respectively. In both cases, the nonuniformity of the field at the nuclei leads formally to an inhomogeneity in both the nuclear magnetization and (through the intereaction with it) the electronic magnetization. The effective Hamiltonian describing the hyperfine interaction is given by

$$\hat{\mathscr{H}}=\sum_i \hat{\mathbf{S}}_i A_i \hat{\mathbf{I}}_i,$$

where $\hat{\mathbf{S}}_i$ is the spin of the electron shell of the atom and $\hat{\mathbf{I}}_i$ is the spin of the nucleus.

In the case of macroscopic inhomogeneities ($r_\alpha \ll r_0$), we can consider local regions in a specimen of intermediate size r_b. Since $r_\alpha \ll r_b$, these regions do not interact with one another and, since $r_b \ll r_0$, all the quantities in the expression for $\hat{\mathscr{H}}$ can be regarded as independent of position within each such region. The susceptibility (3) then corresponds to the local susceptibility of each such region, and the susceptibility of the entire specimen can be obtained by taking the average of (3) with a distribution function $g(H_n)$:

$$\chi=\int\frac{\chi_e g(H_n)\,dH_n}{1-(qA)^2\chi_e\chi_n}. \tag{5}$$

In the other limiting case, which involves the microscopic inhomogeneities ($r_0 \ll r_\alpha$), we again consider local regions in a specimen of intermediate size r_b (in this case, $r_0 \ll r_b \ll r_\alpha$), and average $\hat{\mathscr{H}}$ over the local region. Since $r_b \ll r_\alpha$, the electron magnetization in a region of this kind is strongly dependent on the exchange interaction. We shall therefore assume that it is approximately constant and, since $r_b \gg r_0$, we shall divide the nuclear system into isochromatic regions with dimensionless magnetization $\mu(H_n)$ given by

$$\mu(H_n)=N\mu_I^2 H_n g(H_n)/3kT, \tag{6}$$

where μ_I is the magnetic moment of the nucleus and N is the concentration of the nuclei.[10] The macroscopic energy density is, therefore, given by

$$\mathscr{H}=\langle\hat{\mathscr{H}}\rangle=\mathbf{M}\int A(H_n)\mu(H_n)\,dH_n. \tag{7}$$

This shows that the electron magnetization M interacts with the resultant field $\int A\mu(H_n)dH_n$ of the nuclear isochromatic regions.

The equation of motion corresponding to this interaction Hamiltonian contains the effective magnetic field

$$\mathbf{H}_M=-\int A\mu(H_n)\,dH_n,\quad \mathbf{H}_\mu'=-A\mathbf{M}, \tag{8}$$

and the expression for susceptibility assumes the form

$$\chi=\chi_e\Big/\left[1-\chi_e\int (qA)^2\chi_n g(H_n)\,dH_n\right]. \tag{9}$$

In general, this expression is very different from (5), but in the case of a weak nuclear signal, i.e., when $\omega_q^2/4\Gamma_e\Gamma_n \ll 1$, we can expand the denominators in both formulas and, if we retain only the first term, the result is the same expression, namely,

$$\chi=\chi_e\left[1+\chi_e\int (qA)^2\chi_n g(H_n)\,dH_n\right]. \tag{10}$$

In most cases of importance in practice, the variances of q and A are small, and the average values of these quantities can be taken outside the integral sign. With a sufficient degree of precision, we can therefore use the expression

$$\chi\approx\chi_e[1+(q_0A_0)^2\chi_e\tilde{\chi}_n]. \tag{11}$$

Here

$$\tilde{\chi}_n=\int\chi_n g(H_n)\,dH_n$$

is the integrated nuclear susceptibility and q_0 and A_0 are the average values of q and A. If the inhomogeneous broadening of the NMR line is small in comparsion with the homogeneous broadening, the integrated susceptibility $\tilde{\chi}_n$ is not very different from χ_n. When the opposite inequality is valid, the integrated nuclear susceptibility is wholly determined by the form of the function $g(H_n)$.

The abosrption of the high-frequency field energy in the case of the weak nuclear signal is described by

$$P=\frac{h^2\omega}{2}\frac{Q}{t^2+1}\left[1+(q_0A_0)^2Q\frac{t^2-1}{t^2+1}\tilde{\chi}_n''(\omega)+2(q_0A_0)^2Q\frac{t}{t^2+1}\tilde{\chi}_n'(\omega)\right], \tag{12}$$

where $Q=\chi_e^0\omega_e^2/2\Gamma_e\omega$. This expression is valid for any relationship between ω, ω_e and ω_n. When ω is close to ω_e, we can neglect the small terms $\sim t\tilde{\chi}_n$ and t^4, and obtain the following simple expression which is convenient in the analysis of ENMR experiments:

$$P={}^1/_2h^2\omega Q[1-t^2-A_0^2Q\tilde{\chi}_n''(\omega)]. \tag{13}$$

It is clear therefore that the ENMR spectrum can be used to deduce the imaginary part of the integrated nuclear susceptibility $\tilde{\chi}_n''$.

We must now consider the phenomena that should be observed when the region of overlap of the nuclear and electron resonances is field-scanned. We again return to the expression (3) for the susceptibility. Since NMR frequency ω_n is practically independent of the field H, field-scanning should result in the single-mode FMR or AFMR signal. Accordingly, for a fixed value of the frequency ω, the absorption line $P(H)=\omega\chi''h^2/2$ describes an electron resonance with a single maximum. When ω approaches ω_n, the FMR and AFMR amplitude $P_{\max}$ is reduced and the linewidth ΔH is increased. At the point where $\omega=\omega_n$, the amplitude of the electron resonance is then reduced by the factor $1+\omega_q^2/4\Gamma_e\Gamma_n$.

The most interesting effect in the overlap region is the shift of the FMR and AFMR resonance field H_0. If we equate the derivative $\partial P/\partial H$ to zero, we obtain the following algebraic equation for the resonance field H_0 in the case of the ferromagnetic material:

$$\gamma_e^2[M/\chi_{ex}^0(H_0)+H_\Delta][M/\chi_{ey}^0(H_0)]=\omega^2 \tag{14}$$

and

$$\gamma_e^2[H_0(H_0+H_D)+H_EH_\Delta]=\omega^2 \tag{15}$$

in the case of the antiferromagnetic material, where H_D is the Dzyaloshinskiĭ field. The influence of the nuclear system on H_0 is manifest by the appearance of the effective field H_Δ given by

$$H_\Delta(\omega)=H_n A[\chi_n^0-\chi_n'(\omega)]. \tag{16}$$

The first term in this expression describes the longitudinal (static) hyperfine field experienced by the electron system, i.e., $A\mu$. The second term is due to the fact that the transverse component $A\mu\perp$ of the hyperfine field contains the component H⊥ which, in turn, is proportional to the transverse component of the electron magnetization and is given by

$$\mathbf{H}_\perp=-A\chi_n'(-A\mathbf{M}_\perp)=A^2\chi_n'\mathbf{M}_\perp. \tag{17}$$

On the other hand, it is well known that an effective field of the form βM⊥, (i.e., a field involving anisotropy in the plane of precession) leads to the appearance of the term

$$H_\Delta=-\beta M=-H_n A\chi_n' \tag{18}$$

in the expression for ω_e.

Let us consider (16) in greater detail. When $\omega \gg \omega_n$, the second term in this expression is small, and H_Δ is determined by the static hyperfine field which is easily observed in the AFMR because of the presence of the exchange amplification.[15] In the overlap region, H_Δ is determined by the second term in (16), i.e., by the real part of the nuclear susceptibility. Finally, when $\omega \to 0$, we have $H_\Delta \to 0$. The remarkable fact is that the shift of the FMR and AFMR resonance field, δH_0, is independent of Γ_e and, consequently, independent of whether the eigenfrequencies repel or cross. Contrary to the generally adopted view (see, for example, Turov and Petrov[11]), the function $H_0(\omega)$ has no relation to the behavior of the eigenfrequencies of the system. Figure 1 shows a schematic representation of H_0 as a function of frequency (curve 1). For comparison, it also shows graphs of the eigenfrequencies of the electron vibrations for $\Gamma_e \ll \omega_q \ll \omega_n$ (curve 2) and $\omega_q \ll \Gamma_e \ll \omega_n$ (curve 3). The dashed curve corresponds to the absence of the nuclear system. We note that analogous effects should be observed in the case of the interaction of FMR and AFMR with any other resonance whose frequency is independent of the internal magnetic field.

In the case of the weak nuclear signal, the reduction in amplitude and the broadening of the electron resonance in the overlap region are small effects. The influence of the nuclear system should then be reflected mostly in the shift of the FMR and AFMR resonance field. When the nonuniformity of the field at the nucleus is taken into account, and if we use (12), we obtain

$$H_\Delta(\omega)=H_{n0}A_0[\chi_n^0-\hat{\chi}_n'(\omega)], \tag{19}$$

where H_{n0} is the average value of H_n. Hence, it is clear

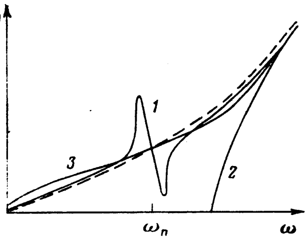

FIG. 1. FMR (AFMR) resonance field H_0 as a function of frequency ω in the case of interaction with NMR (curve 1) and in the absence of this interaction (broken curve). The eigenfrequencies are plotted for $\Gamma_e \ll \omega_q \ll \omega_n$ (curve 2) and $\omega_q \ll \Gamma_e \ll \omega_n$ (curve 3).

that, if we use the resonance-field shift we can determine the real part of the integrated nuclear susceptibility $\hat{\chi}_n'(\omega)$.

In the ferromagnetic films used in our experiments, the FMR line was found to be strongly broadened by the inhomogeneities of the anisotropy field.[16] We shall therefore conclude this section by estimating the influence of anisotropy inhomogeneity on the absorption line shape. For simplicity, we shall use the rectangular distribution function for the anisotropy field $\varphi(H_k)$ with width $\Delta H^* \gg \Delta H$. Averaging (12) with the distribution function $\varphi(H_h)$, we obtain the following expression for the ferromagnetic plate

$$P=\tfrac{1}{2}h^2\omega Q^*[\tfrac{1}{2}\pi-lt_0^2-A_0^2Q^*(1+t_0^2) \times\hat{\chi}_n''(\omega)+2lA_0^2Q^*t_0\hat{\chi}_n'(\omega)]. \tag{20}$$

Here

$$t_0=(\omega_{e0}^2-\omega^2)/2\Gamma_c\omega,\quad t_0\ll 1,\qquad l=\Delta H/\Delta H^*,\quad Q^*=lQ, \tag{21}$$

and ω_{e0} is the average FMR frequency.

Neglecting small terms $\sim t\hat{\chi}_n$, again to within the factor $\pi/2$, we obtain the expression given by (13) in which, however, Q is replaced by Q^*. Hence, it is clear that the anisotropy inhomogeneity leads to a reduction in the relative amplitude of the nuclear signal in the case of ENMR by a factor of $\Delta H^*/\Delta H$. The amplitude of the nuclear signal is, therefore, determined by the effective FMR half-width $\Gamma_e\Delta H^*/\Delta H$. On the other hand, it follows from (20) that the expression given by (16) is unaffected. This means that anisotropy inhomogeneity has no effect on the shift of the FMR resonance field.

3. EXPERIMENT

The experiments in the region of overlap between NMR and FMR were performed with thin cobalt-permalloy films. The FMR frequency was reduced down to the value of the NMR frequency by applying an external field parallel to the plane of the film in the direction of difficult magnetization. For this situation,

$$\chi_{ex}^0=M/(H-H_\kappa),\quad \chi_{cy}^0=1/4\pi,\qquad \omega_e=\gamma_e[4\pi M(H-H_\kappa)]^{1/2},\quad \omega_q^2=4\pi\gamma_c^2 H_n\mu,\quad \delta H_0=-H_\Delta. \tag{22}$$

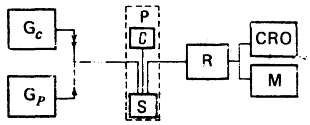

FIG. 2. Block diagram of the experimental setup: G_c—continuous signal generator; G_p—pulse generator; P—probe; C—capacitor; S—coil and specimen; R—receiver; CRO—oscillograph; M—measuring instrument.

The measurements were performed with the composite system illustrated in Fig. 2, which was used to determine resistive losses in the specimen and to observe the nuclear spin echo. The latter was produced by introducing the radiofrequency pulse generator G_p. The spin-echo signal from the probe P was amplified by the receiving system R and displayed on the screen of the oscillograph CRO. ENMR was observed by connecting the continuous signal generator G_c to the probe. In the case of frequency scanning, the absorption P_1 of energy in the specimen in the overlap field ($\mathbf{H} \perp \mathbf{h}$ and $\omega_e(H) = \omega_n$) is compared with the absorption P_0 in a strong field $\mathbf{H} \parallel \mathbf{h}$, where it is practically independent of frequency. Measurements of $P(\omega)$ are then expressed in relative units: $P(\omega) = P_1(\omega)/P_0$. The use of a high-gain receiving system enabled us to work with very low values of the high frequency field, which ensured that the nuclear spin system was well away from saturation. The oscillograph was used to facilitate the search for the signal, and the measurements themselves were made with a high-precision pointer instrument. The probe was a resonant circuit consisting of the flat multiturn coil S into which the film under investigation was inserted, and a tuning capacitor C connected to the coil by a cable of length l ($\frac{1}{4}\lambda_{max} < l < \frac{1}{2}\lambda_{min}$), where λ is the working wavelength.[17] This enabled us to increase the number of turns in the coil and, consequently, the sensitivity and uniformity of the high-frequency field. The excitation of the high-frequency oscillations in the circuit was produced by the series method, using the voltage induced in the outer braid of the shorted end of the generator cable. This scheme ensures minimum parasitic transmission of the generator signal to the receiving system. To observe ENMR, the conditions $\mathbf{H} \perp \mathbf{H}_k$ and $\mathbf{H} \perp \mathbf{h}$ must be strictly satisfied since a slight departure by a degree or so of even one of these fields from these conditions leads to a substantial reduction in the nuclear signal at ENMR. This gives rise to additional difficulties in the comparsion of ENMR and spin-echo signals obtained in different systems. The use of a composite system and a common probe facilitates reliable comparison of the results obtained by experiments under pulse and stationary conditions.

ENMR was observed by frequency scanning in films with different amounts of cobalt, including pure cobalt films. Well-defined ENMR signals could be obtained only for sufficiently homogeneous films with minimum hysteresis loop area for magnetization along the difficult axis. When the temperature is reduced from room to liquid-nitrogen values in the case of the cobalt-permalloy films, it is found that Γ_e is reduced, so that the relative amplitude of the nuclear signal $\sim\mu/\Gamma_e$ increases substantially. For cobalt films, on the other hand, Γ_e is found to increase (in fact, more rapidly than μ) and the amplitude of the nuclear signal decreases. (In this section, Γ_e and Γ_n are interpreted as the effective FMR and NMR half-widths corrected for inhomogeneity). In our experiments, the relative amplitude of the nuclear signal (2) did not exceed 20%, indicating that we were working under the weak nuclear signal conditions. The shift of the FMR field, δH_0, was observed for a much broader class of specimens than ENMR. The degree of uniformity can now be much less stringent, clearly, because δH_0 does not depend on Γ_e.

As an example, let us consider in greater detail the experimental results obtained for a specimen with a simple single-peak NMR spectrum. Figure 3a shows the ENMR spectrum recorded by frequency scanning for $\omega_e(H)/2\pi = \omega_n/2\pi = 210$ MHz. The broken lines shows the smooth FMR peak in the absence of the nuclear system. On the scale of this figure, this is practically a straight line. The inverted NMR signal is, as already mentioned, proportional to the imaginary part of the nuclear susceptibility, $\Delta P \sim -\hat{\chi}_n''$. When H is varied, the FMR signal is found to shift in frequency, and only the smooth FMR top is observed for $\omega_e(H)/2\pi = 280$ MHz. Figure 3b shows the NMR spectrum A echo (ω), recorded by the spin-echo method. The spectrum A echo (ω) corresponds exactly to the $\hat{\chi}_n''(\omega)$ line, which is a characteristic feature of systems with strong inhomogeneous NMR broadening. Figure 3c shows the resonance FMR field H_0 as a function of frequency. The experiment was performed as follows: a particular frequency ω was fixed and the value of H_0 corresponding to maximum absorption under field scanning was determined. The broken line shows the function $H_0(\omega)$ in the absence of the nuclear system.

Finally, Fig. 3d shows the shift of the NMR field obtained from Fig. 1c and proportional to the real part of the nuclear susceptibility, χ_n'. The graphs of $\hat{\chi}_n'(\omega)$ and $\hat{\chi}_n''(\omega)$ are in good agreement with one another. If we use the method of processing the ENMR spectrum proposed by Ignatchenko *et al.*[11] together with $\Gamma_e/2\pi = 700 \pm 110$ MHz (calculated from the FMR linewidth ΔH) we find that Fig. 3a yields $\mu = 2.4 \pm 0.4 \times 10^{-4}$ G. This agrees to within experimental error with value $\mu = 2.2 \times 10^{-4}$ G, found from the Langevin formula. The maxi-

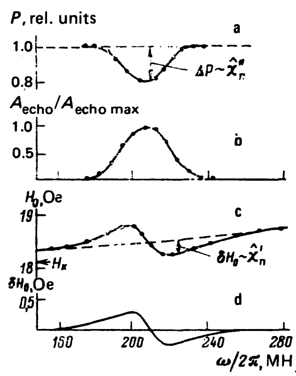

FIG. 3. ENMR spectrum (a) and NMR spectrum recorded by the spin-echo method (b). Frequency dependence of the FMR resonance field (c) and of the shift of the FMR resonance field (d).

mum shift of the FMR field deduced from (19), i.e.,

$$\delta H_0 \approx \omega_n A\mu/4\Gamma_n \approx 0.3\,\mathrm{Oe} \qquad (23)$$

is quite close to the observed value of δH_0. Our experiments thus show that the ENMR method can be an important source of data, and have also demonstrated the shift of the FMR field.

We must now consider the pulse experiments in the NMR-FMR overlap region. As in the experiments described by Pogorelyĭ and Kotov,[5] we observed a sharp increase in the amplitude of the nuclear spin echo as $\omega_e(H) \to \omega_n$ (Fig. 4a). This is obviously connected with an increase in electron susceptibility at the NMR frequency as $\omega_e(H) \to \omega_n$.[9] The most interesting effect is the very fact that the spin echo is observed for ordinary delay times τ between the high-frequency master pulses ($\tau > 10$ μsec), since the characteristic electron-nuclear relaxation time for $\omega_e(H) = \omega_n$ is $\Gamma_\varkappa^{-1} = 4\Gamma_e/\omega_q^2 = 0.09$ μsec. The nuclear spin echo can be observed for $\tau > \Gamma_\varkappa^{-1}$ because under the conditions of microscopic inhomogeneity of the hyperfine field, the electron nuclear relaxation is effective only for short intervals of time during which free precession decays and the spin echo is formed,[10] so that the relative change in the echo amplitude due to electron nuclear relaxation is $\Delta A_{echo}/A_{echo} \lesssim \Gamma_\varkappa/\Gamma_n$, i.e., it does not exceed in order of magnitude the relative amplitude of the nuclear signal in the case of ENMR. The dependence of the echo amplitude on the delay time τ can be approximately represented by an exponential with characteristic time L_2 (for $\omega_e \gg \omega_n$, we have $L_2 = T_2$). Figure 4b shows the function $L_2(H)$ which we have deduced from our experimental data. The magnitude of L_2 is appreciably reduced in the region in which the resonances overlap.

We have also performed another series of experiments in which a preliminary pulse was used to excite the nuclear system and then the usual spin-echo program was introduced after a time τ_0. The dependence of the echo amplitude on τ_0 can also be represented approximately by an exponential with a characteristic time L_1 ($L_1 = T_1$ when $\omega_e \gg \omega_n$). To within experimental error, the relative changes in L_1 and L_2 in the overlap regions are roughly the same (Fig. 4b) but, in absolute magnitude, L_1 exceeds L_2 by more than an order of magnitude. In our opinion, the reduction in L_1 and L_2 in the region of NMR-FMR overlap is connected with the mechanism of the electron nuclear relaxation.[1)]

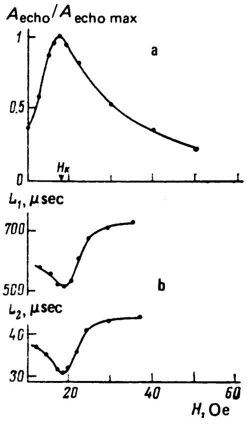

FIG. 4. Spin-echo amplitude as a function of field H (a) and graphs of $L_1(H)$ and $L_2(H)$ (b).

CONCLUSIONS

In conclusion, let us consider separately the situation where the FMR overlapping NMR is scanned by varying the magnetic field, because some misunderstanding has arisen in the literature in this connection. The first paper in which the NMR-FMR overlap was examined experimentally was that by Pogorelyĭ and Kotov,[5] who used field scanning of the resonance, but did not mention this in their paper. They obtained a curve for the resonance field H_0 as a function of frequency, which was similar to curve in Fig. 3c above, and interpreted it qualitatively as a crossing of the eigenfrequencies of the system due to damping. Portis[6] showed that, when damping was taken account, the result was a similar curve, but did not achieve quantitative agreement. Ignatchenko and Tsifrinovich,[8] who predicted theoretically the ENMR phenomenon (with frequency scanning) suggested that Pogorelyĭ and Kotov[5] observed ENMR, but with inadequate resolution. In actual fact, none of these intepretations was correct.

The behavior of the eigenfrequencies of the system does not correspond to the behavior of the $H_0(\omega)$ curve (see Fig. 1 above), and ENMR can be observed only by frequency scanning. This was first confirmed experimentally in our previous paper.[11] The phenomenon observed by Pogorelyi and Kotov, on the other hand, is described by (14) and is of independent interest. As was shown above, this phenomenon can be used to determine the integrated susceptibility of the nuclear system, χ_n', and, therefore, is capable of yielding comparable information to the ENMR method which $\hat{\chi}_n''$. For specimens in which the electron magnetization is highly inhomogeneous, the method based on the recording of the $H_0(\omega)$ curve may be more sensitive than the ENMR method.

1)It would appear that the reduction in L_1 at the overlap point was first observed by Repnikov and Ustinov,[18] but their experiments are not amenable to an unambiguous interpretation.

1E. A. Turov and M. P. Petrov, Yadernyĭ magnitnyĭ rezonans v ferro i antiferromagnetnikakh (Nuclear Magnetic Resonance in Ferro- and Antiferromagnetic Materials), Nauka, M., 1969.
2V. A. Ignatchenko and Yu. A. Kudenko, Radiospektroskopiya tverdogo tela (sb materialov konf., Krasnoyarsk, 1964) [Radiospectroscopy of Solids (Proc. Conf. held at Kransnoyarsk in 1964)], Atomizdat, 1967, p. 181; Izv Akad. Nauk SSSR Ser. Fiz. 30, 77 (1966).
3L. G. Onoprienko, Fiz. Met. Metalloved. 19, 481 (1965).
4E. A. Turov and V. G. Kuleev, Zh. Eskp. Teor. Fiz. 49, 248 (1965). [Sov. Phys. JETP 22, 176 (1966)].
5A. N. Pogorelyĭ and V. V. Kotov, Pis'ma Zh. Eksp. Teor. Fiz. 14, 305 (1971) [JETP Lett. 14, 202 (1971)].
6A. M Portis, AIP Conf. Proc. No 10, Pt. 1, 120 (1972).
7M. N. Botvinko and M. A. Ivanov, Fiz. Tverd. Tela (Leningrad) 15, 1704 (1973) [Sov. Phys. Solid State 15, 1142 (1973)].

[8]V. A. Ignatchenko and V. I. Tsifrinovich, Zh Eksp. Teor. Fiz. 68, 672 (1975) [Sov. Phys. JETP 41, 333 (1975)] 69, 1243 (1975) [Sov. Phys. JETP 42, 635 (1975)] Preprint IFSO-29F, Krasnoyarsk, 1975.
[9]V. I. Tsifrinovich and V. A. Ignatchenko, Zh. Eksp. Teor. Fiz. 72, 803 (1977) [Sov. Phys. JETP 45, 419 (1977)].
[10]V. I. Tsifrinovich, Fiz. Tverd. Tela. Leningrad) 20, No. 6 (1978) [Sov. Phys. Solid State 20, No. 6 (1978)].
[11]V. A. Ignatchenko, N. M. Salanskiĭ, V. K. Mal'tsev, and V. I. Tsifrinovich, Pis'ma Zh. Eksp. Teor. Fiz. 21, 472 (1975) [JETP Lett. 21, 218 (1975)].
[12]V. A. Ignatchenko, V. K. Mal'tsev, and V. I. Tsifrinovich, Fiz. Tverd. Tela (Leningrad) 19, 2036 (1977) [Sov. Phys. Solid State 19, 1191 (1977)].
[13]A. C. Gossard, A. M. Portis, M. Rubinstein, and R. H. Lindquist, Phys. Rev. 138, A1415 (1965).
[14]V. A. Ignatchenko, Zh. Eksp. Teor. Fiz. 54, 303 (1968) [Sov. Phys. JETP 27, 162 (1968).
[15]A. S. Borovik-Romanov, in: Problemy magnetizma (Problems in Magnetism), Nauka, 1972, p. 47.
[16]N. M. Salanskiĭ, V. A. Ignatchenko, and B. P. Khrustalev, in: Fizika magnitnykh plenok (Physics of Magnetic Films), Irkutsk Pedagogical Institute, 1968.
[17]N. M. Salanskiĭ, V. K. Mal'tsev, and E. A. Glozman, Dep. VINITI, No. 918-76, 1976, p. 30.
[18]S. P. Repnikov and V. B. Ustinov, Fiz. Tverd. Tela (Leningrad) 11, 499 (1969) [Sov. Phys. Solid State 11, 395 (1969)].

Translated by S. Chomet

Magnetic susceptibility of transition-metal alloys with the hcp structure

N. V. Volkenshteĭn, É. V. Galoshina, N. B. Gorina, N. L. Korenovskiĭ, V. P. Polyakova, and E. M. Savitskiĭ

Institute of Metal Physics, Ural Scientific Center of the Academy of Sciences of the USSR, Sverdlovsk
(Submitted 7 March 1978)
Zh. Eksp. Teor. Fiz. 75, 228–233 (July 1978)

An investigation was made of the angular dependences of the magnetic susceptibility of Ru–Nb, Re–W, and Os–Re alloy single crystals in the hcp structure range. The published values of the electron specific heat were used to estimate the spin susceptibility. The principal values of the orbital component of the susceptibility ($\chi_{\parallel orb}$ and $\chi_{\perp orb}$) were determined on the assumption of isotropy of the spin contribution to the susceptibility. It was found that alloying had the following effects: the orbital contributions and the anisotropy $\Delta\chi$ of the susceptibility increased in the case of the Ru–Nb alloys; the spin contribution became greater but the orbital susceptibility and the anisotropy $\Delta\chi$ decreased in the case of the Re–W system; the orbital contributions became greater but $\Delta\chi$ was not affected for Os–Re. It was concluded that the addition of the second metal altered the overlap of the wave functions of the *d* electrons.

PACS numbers: 75.20.Em, 75.30.Gw

Transition metals with the hcp structure can be divided into three groups in accordance with the sign and magnitude of the magnetic susceptibility anisotropy.[1] The first group (Sc, Y) is characterized by negative and moderate values of $\Delta\chi$ ($\Delta\chi = \chi_\parallel - \chi_\perp$). The second group (Ti, Zr, and Hf) has the largest and positive values of $\Delta\chi$. In the case of the third group (Re, Ru, and Os) the difference between the susceptibilites $\Delta\chi$ is negative and minimal. Metals in the first and second groups form practically no alloys with the hcp structure. Only the third group has a limited solid-solution range. Studies of the anisotropy of the magnetic susceptibility of the alloys is of interest because it provides information on the magnetism of weakly magnetic transition metals and its relationship to the electron structure.

We investigated Ru–0.7 wt.% Nb, Re–3 wt.% W, and Os–20 wt.% Re alloys. Single crystals were prepared by zone melting. The magnetic susceptibility was measured by the Faraday method using spherical samples in fields up to 11 kOe between liquid hydrogen and room temperatures. The angular dependences of the magnetic susceptibility were determined and the temperature dependences of χ were found along the principal directions [$\chi_\parallel(T)$ and $\chi_\perp(T)$]. A comparison was made with the magnetic susceptibilities of the corresponding pure metals.

We shall start considering the results by comparing the angular dependences of the susceptibility of the alloys with $\chi(\varphi)$ for the pure metals. In the pure state the magnetic susceptibility is strongest when the magnetic field is perpendicular to the hexagonal axis, i.e., $\Delta\chi = \chi_\parallel - \chi_\perp < 0$. A similar relationship between $\chi_\parallel$ and $\chi_\perp$ is also observed for the alloys: $\chi_\perp > \chi_\parallel$ (Table I).

TABLE I. Electron density (e/a), principal values of magnetic susceptibility ($\chi_\parallel$ and $\chi_\perp$), average magnetic susceptibility of polycrystalline samples [$\chi_{poly} = (\chi_\parallel + 2\chi_\perp)/3$], susceptibility anisotropy ($\Delta\chi = \chi_\parallel - \chi_\perp$), and temperature coefficients of susceptibility ($d\chi_\parallel/dT$, $d\chi_\perp/dT$) of pure metals and alloys.

Alloy	e/a	$\chi_\parallel$ *	$\chi_\perp$ *	χ^*_{poly}	$\Delta\chi$ *	$d\chi_\parallel/dT$ **	$d\chi_\perp/dT$ **
Ru	8	35.2±0.2	44.2±0.2	41.2	−9.0	1.4	1.2
0,7% Nb	7.97	35.8	47.7	43.7	−11.9	1.4	1.6
Re	7	68.3	73.0	69.8	−5.4	3.7	2.0
1,0% W	6.99	69.8	74.1	72.7	−4.3	3.3	2.2
3,0% W	6.97	72.8	74.6	74.0	−1.8	3.7	2.2
Os	8	5.4	12.6	10.2	−7.2	0.8	0.3
10% Re	7.9	10.8	19.7	16.7	−8.9	0.7	0.1
20% Re	7.8	22.7	30.7	28.0	−8.0	0.4	0.35

*Values given in units of 10^{-6} cm^3/mole at 293 °K.
**Coefficients $d\chi_{\parallel,\perp}/dT$ found by linear approximation of dependences $\chi_{\parallel,\perp}(T)$ in the range 150–250 °K, given in units of 10^{-8} cm$^3 \cdot$ mole$^{-1} \cdot$ deg^{-1}.

 0038-5646/78/070114-03$02.40